

# Raman spectroscopy as a promising noninvasive tool in brain cancer detection

Piyush Kumar

*Amity Institute of Biotechnology*

*Amity University Mumbai*

*Bhatan, Post-Somatane, Panvel*

*Navi Mumbai, Maharashtra 410206, India*

*piyush.kaviraj@gmail.com; pkumar@mum.amity.edu*

Received 30 June 2017

Accepted 7 September 2017

Published 27 September 2017

Despite intensive therapy regimen, brain cancers present with a poor prognosis, with an estimated median survival time of less than 15 months in case of glioblastoma. Early detection and improved surgical resections are suggested to enhance prognosis; several tools are being explored to achieve the purpose. Raman spectroscopy (RS), a nondestructive and noninvasive technique, has been extensively explored in brain cancers. This review summarizes RS-based studies in brain cancers, categorized into studies on animal models, *ex vivo* human samples, and *in vivo* human subjects. Findings suggest RS as a promising tool which can aid in improving the accuracy of brain tumor surgery. Further advancements in instrumentation, market-assessment, and clinical trials can facilitate translation of the technology as a noninvasive intraoperative guidance tool.

*Keywords:* Raman spectroscopy; brain cancers; intraoperative; glioma.

## 1. Introduction

Despite intensive therapy regimen, brain cancers still present a poor prognosis. The diagnostic classification of brain tumors is majorly based on the scheme proposed by Bailey and Cushing,<sup>1</sup> and refined by several people,<sup>2,3</sup> including Kernohans and Mabon.<sup>2</sup> The World Health Organization (WHO) took further initiatives and formalized the criteria, which are also frequently updated.<sup>4</sup> Brain cancers arise from the brain cells which are a part of the nervous system. The neuroglial common progenitor

cells differentiate into neuronal and glial progenitor cells which further differentiate to form components of the nervous system, such as neurons, oligodendrocytes, and astrocytes. The two most common brain tumors, medulloblastoma and glioblastoma, arise from the neuronal and glial lineages, respectively. Despite intensive therapy regimen, the survival rates are poor for brain cancers. Patients with WHO grade II and III tumors typically survive > 5 years, and 2–3 years, respectively, while the prognosis for WHO grade IV tumors is variable;

most glioblastoma patients often die within a year,<sup>4</sup> and the median survival time is estimated to be less than 15 months.<sup>5</sup>

The current diagnosis includes a combination of CT scans, magnetic resonance imaging (MRI), and electroencephalogram while the standard treatment, especially in case of gliomas, involves surgical resection along with adjuvant radio- and chemotherapy. However, surgical resection can be a tricky affair as post-surgery residual cancer cells may lead to recurrence while excision of healthy tissues can lead to cognitive deficits in patients.<sup>6,7</sup> Thus, better tools for diagnosis as well as real-time guided surgery are needed for better outcomes. As biochemical changes often precede morphological changes, tools which are sensitive to tissue biochemistry could be more conducive for early diagnosis. The changes in tissue biochemistry are also reflected in the optical properties of the tissues, and thus in the recent decades, optical techniques, especially Raman spectroscopy (RS), have been extensively explored as noninvasive and objective diagnostic tools in several cancers.<sup>8</sup> RS is based on the principle of inelastic or Raman scattering which was experimentally verified by Sir C. V. Raman.<sup>9</sup> Due to minimal interference from water, a major constituent of living organisms, RS can serve as a candidate tool for *in vivo* explorations.

## 2. Methodology

Raman spectra can be acquired from *ex vivo* tissues, biofluids such as serum, as well as *in vivo*. As RS does not need any processing or staining of samples that are required for conventional diagnosis such as histopathology, the samples can be placed on substrates such as aluminium and calcium fluoride, and quality spectra can be acquired in a few seconds. The raw spectra are pre-processed to remove contributions of optical components and other background signal. As minor spectral differences between the diseased and healthy tissues may not be visually apparent, the pre-processed spectra are subjected to multivariate analysis — unsupervised as well as supervised. Principal component analysis (PCA) is one of the most commonly used unsupervised multivariate method while Linear discriminant analysis (LDA) is a commonly used supervised method.<sup>10,11</sup> The supervised methods are usually used to build and train spectral models which can

test unknown spectra. Usually, corresponding histopathological information is used as a reference to build robust spectral models, which in turn are used to test independently obtained spectra for objective diagnosis. The methodologies to apply RS on various biological samples have been reviewed by Butler *et al.*<sup>12</sup>

## 3. Raman Spectroscopy-Based Exploration in Brain Cancers

In this review, the studies which have employed RS to evaluate brain cancers have been categorized as those carried out on animal models, *ex vivo* human tissues, and *in vivo* studies on human subjects.

### 3.1. Animal studies

Animal models often enable the first line *ex vivo* as well as *in vivo* testing of new tools. The earliest RS-based analyses of brain samples were carried out by Tashibu *et al.* and Mizuno *et al.* Tashibu *et al.* investigated relative water concentration in normal and edematous rat brain tissues by analyzing CH and OH groups in the high wavenumber region.<sup>13</sup> The same groups also investigated cytotoxic and vasogenic brain edema rat models.<sup>14</sup> Mizuno *et al.* used Fourier transform (FT) RS to explore rat brain and published spectra of different brain tumors.<sup>15,16</sup> Spectra were acquired from cerebral cortex, caudate-putamen, white matter of the cerebrum, thalamus, and myelin fraction, and identification of gray and white matters was achieved based on higher lipid content in the white matter.<sup>15</sup> These early studies provided the impetus for further research on human biopsy samples which are described in the next section. Animal models were also used to study normal and necrotic brain tissues by Amharref *et al.*<sup>17</sup> Raman microspectroscopy of 15- $\mu\text{m}$ -thick brain sections followed by pseudo color maps were compared with histopathology and biomarkers for Ki-67 and MT1-MMP.

A major innovation that catapulted RS to *in vivo* studies was the development of fiberoptic probes. Koljenovic *et al.* characterized porcine brain tissues using fiber-optic probes<sup>18</sup> and developed least-squares fitting-based multivariate model to discriminate brain structures. The Raman spectra of gray matter and white matter were analyzed and it was shown that gray matter spectra were

dominated by bands associated with proteins, DNA, and phosphatidylcholine while white matter spectra were dominated by cholesterol and sphingomyelin. Fiber optic probes also facilitated the metastasis studies in mouse models. Krafft *et al.*<sup>19</sup> injected melanoma tumor cells into the carotid artery of mice to induce brain metastasis. Serial sections were prepared from whole mouse brains for Fourier transform infrared (FTIR) and Raman imaging, and for histopathological assessment. While metastatic melanoma cells were not observed in the FTIR images, Raman spectra enabled their detection at 785 nm. Kirsch *et al.* also employed melanoma cell injection into the carotid artery of mice to induce brain metastasis. They created a bony window in the mice skull to enable *in vivo* studies using a fiber-optic probe. Cortical and subcortical tumor cell aggregates could be localized with an accuracy of  $\sim 250 \mu\text{m}$ .<sup>20</sup> *In vivo* studies were also carried out by Beljebbar *et al.*, however, they used a microprobe coupled to their spectrometer instead of a fiberoptic probe. A glioblastoma Wistar rat model was used in this study, obtained after injecting a C6 glioma cell suspension into brain cortex, and sequential progression was monitored at days 4, 6, 8, 11, 13, 15, and 20 post tumor injection.<sup>21</sup> Tanahashi *et al.* compared spectra obtained from mouse models of avian sarcoma-based infiltrative glioma cells and tissues to spectra from normal mouse astrocytes and normal tissues and could distinguish the infiltrative tumors using RS.<sup>22</sup>

### 3.2. *Ex vivo* studies (human samples)

*Ex vivo* tissues-based studies have given major insights regarding the nature and composition of healthy and cancerous tissues. Mizuno *et al.* also employed Fourier transform Raman spectroscopy (FTRS) to investigate various human brain tissue samples and reported that spectra from normal but edematous gray and white matter were similar to those from normal rat gray and white matter. Spectra from gliomas, neurinomas, and neurocytoma were observed to be similar to rat gray matter spectra.<sup>16</sup> Koljenovic *et al.* obtained 24 Raman maps from unstained and unfixed cryosections of 20 glioblastoma tissue samples from 20 patients. LDA-based classification model ( $n = 11$  tissues) was evaluated using the remaining nine sections to obtain 100% accuracy. Biochemical differences between necrosis and vital tumor were analyzed using

difference spectra. Necrotic tissues revealed higher cholesterol and cholesterol-ester levels.<sup>23</sup> Krafft *et al.* acquired Raman spectra of major and minor brain lipids to obtain spectral profiles for qualitative as well as quantitative analyses and reported higher levels of lipids in normal tissues, and higher hemoglobin but lower lipid to protein ratios in intracranial tumors; thus RS could be used to distinguish normal and tumor tissues, and to determine the tumor type and grade.<sup>24,25</sup> Koljenovic *et al.* also suggested that similar diagnostic information is present in both the fingerprint and the high wavenumber region.<sup>26</sup> In view of emerging information on relative lipid content in brain tumors, RS and mass spectrometry of lipid extracts from seven human tissue specimen was carried out by Kohler *et al.*<sup>27</sup> Gliomas were characterized by increased water- and decreased lipid-content, and the results were similar to that observed in porcine tissues. Further, RS suggested phosphatidylcholine to cholesterol ratios were elevated in gliomas while mass spectrometry detected higher cholesterol ester with respect to cholesterol, in lipid extracts of gliomas.<sup>27</sup> Rabah *et al.* were the first to study pediatric brain tumor using RS and could distinguish neuroblastoma and ganglioneuroma.<sup>28</sup> Wills *et al.* used fresh and frozen pediatric neuroblastoma and other neural crest tumors and found encouraging classification using RS.<sup>29</sup> Leslie *et al.* employed RS to distinguish pediatric brain neoplasms from normal brain tissue, and similar tumor-types from each other. Spectra from normal brain ( $n = 321$ ), glioma ( $n = 246$ ), and medulloblastoma ( $n = 82$ ) showed an accuracy of 96.9%, 96.7%, and 93.9%, respectively.<sup>30</sup> Meningioma, glioma, and brain metastasis (from 15 patients each) were distinguished with respect to normal brain samples ( $n = 7$ ) by Gajjar *et al.* who used both FTIR and RS to achieve the goal.<sup>31</sup> In the recent years, different types of brain tumors have been explored by several groups, including Aguiar *et al.* (tumors: glioblastoma, medulloblastoma, and meningioma; normal: cerebellum and meninges),<sup>32</sup> Beleites *et al.* (astrocytoma),<sup>33</sup> Kalkanis *et al.* (normal brain, glioblastoma multiforme, and necrosis),<sup>34</sup> Kast *et al.* (normal brain, necrosis, diffusely infiltrating glioma and solid glioblastoma),<sup>35</sup> Kast *et al.* (boundaries of normal gray and white matter, glioblastoma and necrosis).<sup>36</sup> New multivariate methods to obtain a higher accuracy of classification have also been explored. Liu *et al.* employed learning vector quantization neural

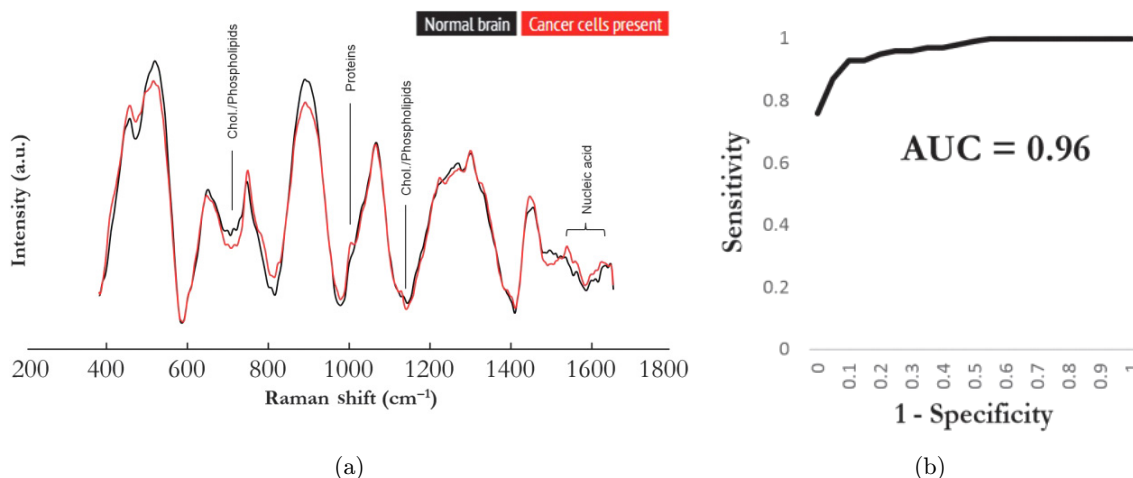


Fig. 1. Raman spectra for discrimination of cancer tissue. (a) Average Raman spectra of *in vivo* measurements for normal brain (all 66 spectra averaged) and tissue containing glioma cancer cells (all 95 spectra averaged). Corresponding molecular contributors are identified for the most significant differences between the spectra for normal and cancer tissues. Chol. = cholesterol. (b) Receiver operating characteristic curve analysis of *in vivo* detection of glioma based on Raman spectroscopy, generated using the boosted trees classification method. AUC = area under the curve. From Ref. 41. Reprinted with permission from AAAS.

network to distinguish white matter and tumors.<sup>37</sup> which yielded a better classification efficiency. In a recent and interesting study, band-wise feature extraction, sound synthesis from Raman spectra and feedback mechanism was employed to achieve classification of spectral data from fixed and paraffin embedded tissue sections. Support vector machine, *K*-nearest neighbor classifier, and LDA were used as classifiers and it was shown that feature extraction, along with dimension reduction may also be used as a potential approach to obtain better results.<sup>38</sup>

### 3.3. *In vivo* studies

Intraoperative *in vivo* brain cancer studies have been reported recently. As mentioned earlier, surgical resection in case of brain cancers is tricky; any residual cancer cells may lead to recurrence while the removal of healthy tissue can result into cognitive impairment. Thus, early resection as well as preserving the functional status of patients is crucial for optimal outcome.<sup>39</sup> Desroches *et al.* explored several confounding factors such as linearity of signal as well as ambient light sources for optimal conditions in an operation theatre. Raman spectra of normal brain, cancer and necrotic tissues ( $n = 10$  patients) demonstrated *in vivo*, real time investigation; necrotic tissues could be distinguished with an accuracy, sensitivity, and specificity of 87%, 84%, and 89%, respectively.<sup>40</sup> The same group

carried out further intraoperative studies using handheld contact probe and could differentiate normal brain from dense cancer with sensitivity and specificity of 93% and 91%, respectively. They could detect previously undetectable diffusely-invasive cancer cells in grade 2–4 glioma patients.<sup>41</sup> Figure 1 shows the mean *in vivo* Raman measurements for normal ( $n = 66$  spectra) and cancerous tissues ( $n = 95$  spectra) along with the major biomolecules contributing significant differences. The same group could obtain improved detection by employing artificial neural network methods.<sup>42</sup> Efficacy of RS has also been compared with MRI which is considered a standard imaging modality. Jermyn *et al.* extended their previous intraoperative study and compared the Raman findings with “T1-contrast-enhanced and T2-weighted MRI sequences”, and reported that RS could detect cancer up to  $\sim 3.7$  cm for T1-contrast enhanced and  $\sim 2.4$  cm for T2 MRI boundary.<sup>43</sup> Recently, researchers from Canada have explored brain needle biopsy and used RS in the high wavenumber region to provide a proof of concept in human subject.<sup>44</sup> A summary of major studies carried out on animal models, *ex vivo* studies on human samples, and *in vivo* studies on human subjects are summarized in Table 1.

## 4. Conclusion

While the above-mentioned studies are encouraging, the translation of RS to clinics and operation

Table 1. Summary of major Raman spectroscopy-based studies.

First author	Year	Highlight
<b>ANIMAL STUDIES</b>		
Tashibu	1990	Relative water concentration in edematous tissues
Mizuno	1992	Spectra from various regions of brain; identification of gray and white matter
Amharref	2007	Normal and necrotic brain study; compared with histopathology and biomarkers
Koljenovic	2007	Characterized porcine brain using fiber-optic probe
Krafft	2007	Metastasis studies using fiber-optic probe
Kirsch	2010	<i>In vivo</i> study using fiber probe
Beljebbar	2010	Microprobe-based study; sequential progression monitored post tumor cell injection
Tanahashi	2014	Diffuse infiltrative glioma mouse model
<b>EX VIVO STUDIES</b>		
Mizuno	1994	FTRS spectra from normal, edematous gray, and white matter
Koljenovic	2002	Raman maps of unstained and unfixed glioblastoma cryosections
Koljenovic	2005	Relatable diagnostic information in fingerprint and high wavenumber regions
Krafft	2005	Spectra of major and minor brain lipids
Rabah	2008	First Raman study on pediatric tumor
Kohler	2009	RS and mass spectrometry of brain lipid extracts
Wills	2009	Pediatric neural crest tumors
Leslie	2012	Pediatric brain neoplasms
Gajjar	2012	Both FTIR and RS used for meningioma, glioma and brain metastasis
Aguiar	2013	RS of different brain regions
Beleites	2011	Astrocytoma
Kalkanis	2014	GBM and necrosis
Kast	2014	Necrosis, diffusely infiltrating glioma and solid glioblastoma
Kast	2015	Boundaries of normal gray/white matter, glioblastoma, and necrosis
Liu	2016	Learning vector quantization of neural network to distinguish white matter and tumor
Stables	2017	Feature driven classification in real time
<b>IN VIVO STUDIES</b>		
Desroches	2015	Explored confounding factors and ambient light sources for optimal conditions in an operation theatre
Jermyn	2015	Handheld device mediated intraoperative study to distinguish diffusively invasive cancer cells
Jermyn	2016	Use of artificial neural network methods for improved detection
Jermyn	2016	RS findings compared with MRI to show better detection
Desroches	2017	Brain needle biopsy analyzed in high wavenumber region

Notes: (FTIR: Fourier-transform infrared spectroscopy; RS: Raman spectroscopy; FTRS: Fourier transform Raman spectroscopy; GBM: Glioblastoma multiforme; MRI: Magnetic resonance imaging).

theatres needs further efforts in terms of developments in instrumentation as well as improved algorithms to acquire large number of spectra with better signal-to-noise ratio, in a clinically implementable time, on a real-time basis. Advancements over RS, including stimulated RS and Coherent Anti-Stokes Raman Scattering have shown encouraging outcomes in brain cancer diagnosis.<sup>45–51</sup> Further, market-assessment and safety studies, followed by clinical trials are needed to advance the technology as an intraoperative guidance tool. In conclusion, RS, as shown by several recent reports, is a promising tool which can aid in improving the accuracy of brain tumor diagnosis and surgical procedures.

## Acknowledgment

I would like to thank Dr. Aditi Sahu, MSKCC, New York, for editorial makeover.

## References

1. P. Bailey, H. Cushing, "A classification of the tumors of the glioma group on a histogenetic basis with a correlated study of prognosis," J. B. Lippincott Co., Philadelphia (1926).
2. J. W. Kernohan, R. Mabon, "A simplified classification of the gliomas," *Proc. Staff Meetings, Mayo Clinic* (1949).
3. N. Ringertz, "Grading of gliomas," *APMIS* **27**, 51–64 (1950).



4. D. N. Louis, H. Ohgaki, O. D. Wiestler, W. K. Cavenee, P. C. Burger, A. Jouvet, B. W. Scheithauer, P. Kleihues, "The 2007 WHO classification of tumours of the central nervous system," *Acta Neuropathol.* **114**, 97–109 (2007).
5. K. R. Lamborn, W. K. A. Yung, S. M. Chang, P. Y. Wen, T. F. Cloughesy, L. M. DeAngelis, H. I. Robins, F. S. Lieberman, H. A. Fine, K. L. Fink, L. Junck, L. Abrey, M. R. Gilbert, M. Mehta, J. G. Kuhn, K. D. Aldape, J. Hibberts, P. M. Peterson, M. D. Prados, N. A. B. T. Consortium, "Progression-free survival: An important end point in evaluating therapy for recurrent high-grade gliomas," *Neuro-Oncol.* **10**, 162–170 (2008).
6. W. Stummer, J.-C. Tonn, H. M. Mehdorn, U. Nestler, K. Franz, C. Goetz, A. Bink, U. Pichlmeier, "Counterbalancing risks and gains from extended resections in malignant glioma surgery: A supplemental analysis from the randomized 5-aminolevulinic acid glioma resection study: Clinical article," *J. Neurosurg.* **114**, 613–623 (2011).
7. I.-F. Talos, K. H. Zou, L. Ohno-Machado, J. G. Bhagwat, R. Kikinis, P. M. Black, F. A. Jolesz, "Supratentorial low-grade glioma resectability: Statistical predictive analysis based on anatomic MR features and tumor characteristics 1," *Radiology* **239**, 506–513 (2006).
8. I. Pence, A. Mahadevan-Jansen, "Clinical instrumentation and applications of Raman spectroscopy," *Chem. Soc. Rev.* **45**, 1958–1979 (2016).
9. C. V. Raman, K. S. Krishnan, "A new type of secondary radiation," *Nature* **121**, 501–502 (1928).
10. H. Abdi, L. J. Williams, "Principal component analysis," *Wiley Interdiscip. Rev. Comput. Stat.* **2**, 433–459 (2010).
11. K. Varmuza, P. Filzmoser, *Introduction to Multivariate Statistical Analysis in Chemometrics*, CRC Press (2009).
12. H. J. Butler, L. Ashton, B. Bird, G. Cinque, K. Curtis, J. Dorney, K. Esmonde-White, N. J. Fullwood, B. Gardner, P. L. Martin-Hirsch, "Using Raman spectroscopy to characterize biological materials," *Nat. Protoc.* **11**, 664–687 (2016).
13. K. Tashibu, "Analysis of water content in rat brain using Raman spectroscopy," *No to Shinkei = Brain and Nerve* **42**, 999–1004 (1990).
14. T. Kitajima, K. Tashibu, S. Tani, A. Mizuno, N. Nakamura, "Analysis of water content in young rats brain edema by Raman spectroscopy," *No to Shinkei = Brain and Nerve* **45**, 519–524 (1993).
15. A. Mizuno, T. Hayashi, K. Tashibu, S. Muraishi, K. Kawauchi, Y. Ozaki, "Near-infrared FT-Raman spectra of the rat brain tissues," *Neurosci. Lett.* **141**, 47–52 (1992).
16. A. Mizuno, H. Kitajima, K. Kawauchi, S. Muraishi, Y. Ozaki, "Near-infrared Fourier transform Raman spectroscopic study of human brain tissues and tumours," *J. Raman Spectrosc.* **25**, 25–29 (1994).
17. N. Amharref, A. Beljebbar, S. Dukic, L. Venteo, L. Schneider, M. Pluot, M. Manfait, "Discriminating healthy from tumor and necrosis tissue in rat brain tissue samples by Raman spectral imaging," *Biochim. Biophys. Acta Biomembr.* **1768**, 2605–2615 (2007).
18. S. Koljenovic, T. Bakker Schut, R. Wolthuis, A. Vincent, G. Hendriks-Hagevi, L. Santos, J. Kros, G. Puppels, "Raman spectroscopic characterization of porcine brain tissue using a single fiber-optic probe," *Anal. Chem.* **79**, 557–564 (2007).
19. C. Krafft, M. Kirsch, C. Beleites, G. Schackert, R. Salzer, "Methodology for fiber-optic Raman mapping and FTIR imaging of metastases in mouse brains," *Anal. Bioanal. Chem.* **389**, 1133–1142 (2007).
20. M. Kirsch, G. Schackert, R. Salzer, C. Krafft, "Raman spectroscopic imaging for *in vivo* detection of cerebral brain metastases," *Anal. Bioanal. Chem.* **398**, 1707–1713 (2010).
21. A. Beljebbar, S. Dukic, N. Amharref, M. Manfait, "Ex vivo and in vivo diagnosis of C6 glioblastoma development by Raman spectroscopy coupled to a microprobe," *Anal. Bioanal. Chem.* **398**, 477–487 (2010).
22. K. Tanahashi, A. Natsume, F. Ohka, H. Momota, A. Kato, K. Motomura, N. Watabe, S. Muraishi, H. Nakahara, Y. Saito, I. Takeuchi, T. Wakabayashi, "Assessment of tumor cells in a mouse model of diffuse infiltrative glioma by Raman spectroscopy," *BioMed. Res. Int.* **2014**, 860241 (2014).
23. S. Koljenovic, L. Choo-Smith, T. C. Bakker Schut, J. M. Kros, H. J. van den Berge, G. J. Puppels, "Discriminating vital tumor from necrotic tissue in human glioblastoma samples by Raman microspectroscopy," *Microsc. Microana.* **8**, 444–445 (2002).
24. C. Krafft, L. Neudert, T. Simat, R. Salzer, "Near infrared Raman spectra of human brain lipids," *Spectrochim. Acta A, Mole. Biomole. Spectrosc.* **61**, 1529–1535 (2005).
25. C. Krafft, S. B. Sobottka, G. Schackert, R. Salzer, "Near infrared Raman spectroscopic mapping of native brain tissue and intracranial tumors," *Analyst* **130**, 1070–1077 (2005).
26. S. Koljenovic, T. B. Schut, R. D. Wolthuis, B. De Jong, L. Santos, P. J. Caspers, J. M. Kros, G. J. Puppels, "Tissue characterization using high wave number Raman spectroscopy," *J. Biomed. Opt.* **10**, 031116–03111611 (2005).
27. M. Köhler, S. Machill, R. Salzer, C. Krafft, "Characterization of lipid extracts from brain tissue

- and tumors using Raman spectroscopy and mass spectrometry," *Analy. Bioanal. Chem.* **393**, 1513–1520 (2009).
28. R. Rabah, R. Weber, G. K. Serhatkulu, A. Cao, H. Dai, A. Pandya, R. Naik, G. Auner, J. Poulik, M. Klein, "Diagnosis of neuroblastoma and ganglioneuroma using Raman spectroscopy," *J. Pediatr. Surg.* **43**, 171–176 (2008).
  29. H. Wills, R. Kast, C. Stewart, R. Rabah, A. Pandya, J. Poulik, G. Auner, M. D. Klein, "Raman spectroscopy detects and distinguishes neuroblastoma and related tissues in fresh and (banked) frozen specimens," *J. Pediatr. Surg.* **44**, 386–391 (2009).
  30. D. G. Leslie, R. E. Kast, J. M. Poulik, R. Rabah, S. Sood, G. W. Auner, M. D. Klein, "Identification of pediatric brain neoplasms using Raman spectroscopy," *Pediatr. Neurosurg.* **48**, 109–117 (2012).
  31. K. Gajjar, L. D. Heppenstall, W. Pang, K. M. Ashton, J. Trevisan, I. I. Patel, V. Llabjani, H. F. Stringfellow, P. L. Martin-Hirsch, T. Dawson, F. L. Martin, "Diagnostic segregation of human brain tumours using Fourier-transform infrared and/or Raman spectroscopy coupled with discriminant analysis," *Anal. Methods: Adv. Methods Appl.* **5**, 89–102 (2012).
  32. R. P. Aguiar, L. Silveira Jr, E. T. Falcao, M. T. T. Pacheco, R. A. Zângaro, C. A. Pasqualucci, "Discriminating neoplastic and normal brain tissues in vitro through Raman spectroscopy: A principal components analysis classification model," *Photomed. Laser Surg.* **31**, 595–604 (2013).
  33. C. Beleites, K. Geiger, M. Kirsch, S. B. Sobottka, G. Schackert, R. Salzer, "Raman spectroscopic grading of astrocytoma tissues: Using soft reference information," *Analy. Bioanal. Chem.* **400**, 2801–2816 (2011).
  34. S. N. Kalkanis, R. E. Kast, M. L. Rosenblum, T. Mikkelsen, S. M. Yurgelevic, K. M. Nelson, A. Raghunathan, L. M. Poisson, G. W. Auner, "Raman spectroscopy to distinguish grey matter, necrosis, and glioblastoma multiforme in frozen tissue sections," *J. Neuro-oncol.* **116**, 477 (2014).
  35. R. E. Kast, G. W. Auner, M. L. Rosenblum, T. Mikkelsen, S. M. Yurgelevic, A. Raghunathan, L. M. Poisson, S. N. Kalkanis, "Raman molecular imaging of brain frozen tissue sections," *J. Neuro-oncol.* **120**, 55 (2014).
  36. R. Kast, G. Auner, S. Yurgelevic, B. Broadbent, A. Raghunathan, L. M. Poisson, T. Mikkelsen, M. L. Rosenblum, S. N. Kalkanis, "Identification of regions of normal grey matter and white matter from pathologic glioblastoma and necrosis in frozen sections using Raman imaging," *J. Neuro-oncol.* **125**, 287 (2015).
  37. T. Liu, C. Chen, X. Shi, C. Liu, "Evaluation of Raman spectra of human brain tumor tissue using the learning vector quantization neural network," *Laser Phys.* **26**, 055606 (2016).
  38. R. Stables, G. Clemens, H. J. Butler, K. M. Ashton, A. Brodbelt, T. P. Dawson, L. M. Fullwood, M. D. Jenkinson, M. J. Baker, "Feature driven classification of Raman spectra for real-time spectral brain tumour diagnosis using sound," *Analyst* **142**, 98–109 (2017).
  39. N. Sanai, M.-Y. Polley, M. W. McDermott, A. T. Parsa, M. S. Berger, "An extent of resection threshold for newly diagnosed glioblastomas," *J. Neurosurg.* **115**, 3–8 (2011).
  40. J. Desroches, M. Jermyn, K. Mok, C. Lemieux-Leduc, J. Mercier, K. St-Arnaud, K. Urmey, M.-C. Guiot, E. Marple, K. Petrecca, "Characterization of a Raman spectroscopy probe system for intraoperative brain tissue classification," *Biomed. Opt. Express* **6**, 2380–2397 (2015).
  41. M. Jermyn, K. Mok, J. Mercier, J. Desroches, J. Pichette, K. Saint-Arnaud, L. Bernstein, M.-C. Guiot, K. Petrecca, F. Leblond, "Intraoperative brain cancer detection with Raman spectroscopy in humans," *Sci. Transl. Med.* **7**, 274ra19–274ra19 (2015).
  42. M. Jermyn, J. Desroches, J. Mercier, M.-A. Tremblay, K. St-Arnaud, M.-C. Guiot, K. Petrecca, F. Leblond, "Neural networks improve brain cancer detection with Raman spectroscopy in the presence of operating room light artifacts," *J. Biomed. Opt.* **21**, 094002–094002 (2016).
  43. M. Jermyn, J. Desroches, J. Mercier, K. St-Arnaud, M.-C. Guiot, F. Leblond, K. Petrecca, "Raman spectroscopy detects distant invasive brain cancer cells centimeters beyond MRI capability in humans," *Biomed. Opt. Express* **7**, 5129–5137 (2016).
  44. J. Desroches, M. Jermyn, M. Pinto, F. Picot, M.-A. Tremblay, S. Obaid, M.-C. Guiot, K. Petrecca, C. B. Wilson, F. Leblond, "High wavenumber Raman spectroscopy to improve diagnostic yield of brain needle biopsies," in *Optics in the Life Sciences Congress* Optical Society of America, San Diego, California (2017).
  45. O. Uckermann, R. Galli, S. Tamosaityte, E. Leipnitz, K. D. Geiger, G. Schackert, E. Koch, G. Steiner, M. Kirsch, "Label-free delineation of brain tumors by coherent anti-Stokes Raman scattering microscopy in an orthotopic mouse model and human glioblastoma," *PLoS One* **9**, e107115 (2014).
  46. M. Ji, D. A. Orringer, C. W. Freudiger, *Sci. Transl. Med.* **5**, 201ra119 (2013).
  47. J. N. Bentley, M. Ji, X. S. Xie, D. A. Orringer, "Real-time image guidance for brain tumor surgery through stimulated Raman scattering microscopy," *Expert Rev. Anticancer Ther.* **14**, 359–361 (2014).
  48. R. Galli, O. Uckermann, A. Temme, E. Leipnitz, M. Meinhardt, E. Koch, G. Schackert, G. Steiner, M.

- Kirsch, "Assessing the efficacy of coherent anti-Stokes Raman scattering microscopy for the detection of infiltrating glioblastoma in fresh brain samples," *J. Biophoton.* **10**, 404–414 (2017).
49. M. Ji, S. Lewis, S. Camelo-Piragua, S. H. Ramkissoon, M. Snuderl, S. Venneti, A. Fisher-Hubbard, M. Garrard, D. Fu, A. C. Wang, "Detection of human brain tumor infiltration with quantitative stimulated Raman scattering microscopy," *Sci. Transl. Med.* **7**, 309ra163–309ra163 (2015).
50. S. Lewis, D. Orringer, "Detection of brain tumors using stimulated Raman scattering microscopy," *Deep Imaging in Tissue and Biomedical Materials: Using Linear and Nonlinear Optical Methods*, CRC Press **413** (2017). ISBN: 1351797395, 9781351797399.
51. Y. Zhou, C.-H. Liu, Y. Pu, G. Cheng, X. Yu, L. Zhou, D. Lin, K. Zhu, R. R. Alfano, "Resonance Raman Spectroscopy of human brain metastasis of lung cancer analyzed by blind source separation," in *Proc. SPIE Proceedings Volume 10051, Neural Imaging and Sensing*; 100511I (2017), doi: 10.1117/12.2254465.